Supporting Information

Host-Guest Complexation of a Lipoic Acid Conjugate of Calix[4]arene with Pyridinium Moiety on Gold Nanorods for Mitochondrial Tracking followed by Cytotoxicity in HeLa Cells under 633 nm Laser Light

Rahul Nag[a], Ravinder Kandi[b] and Chebrolu Pulla Rao[*]

[a,b,]Bioinorganic Laboratory, Department of Chemistry, Indian Institute of Technology Bombay, Powai, Mumbai – 400 076, India, E-mail: nrahul@iitb.ac.in[a], bioravinder@gmail.com[b] cprao@iitb.ac.in[*]*

The supporting information file contains 19 pages, 16 figures and 1 table.

Contents

S1. Spectra for P_3.

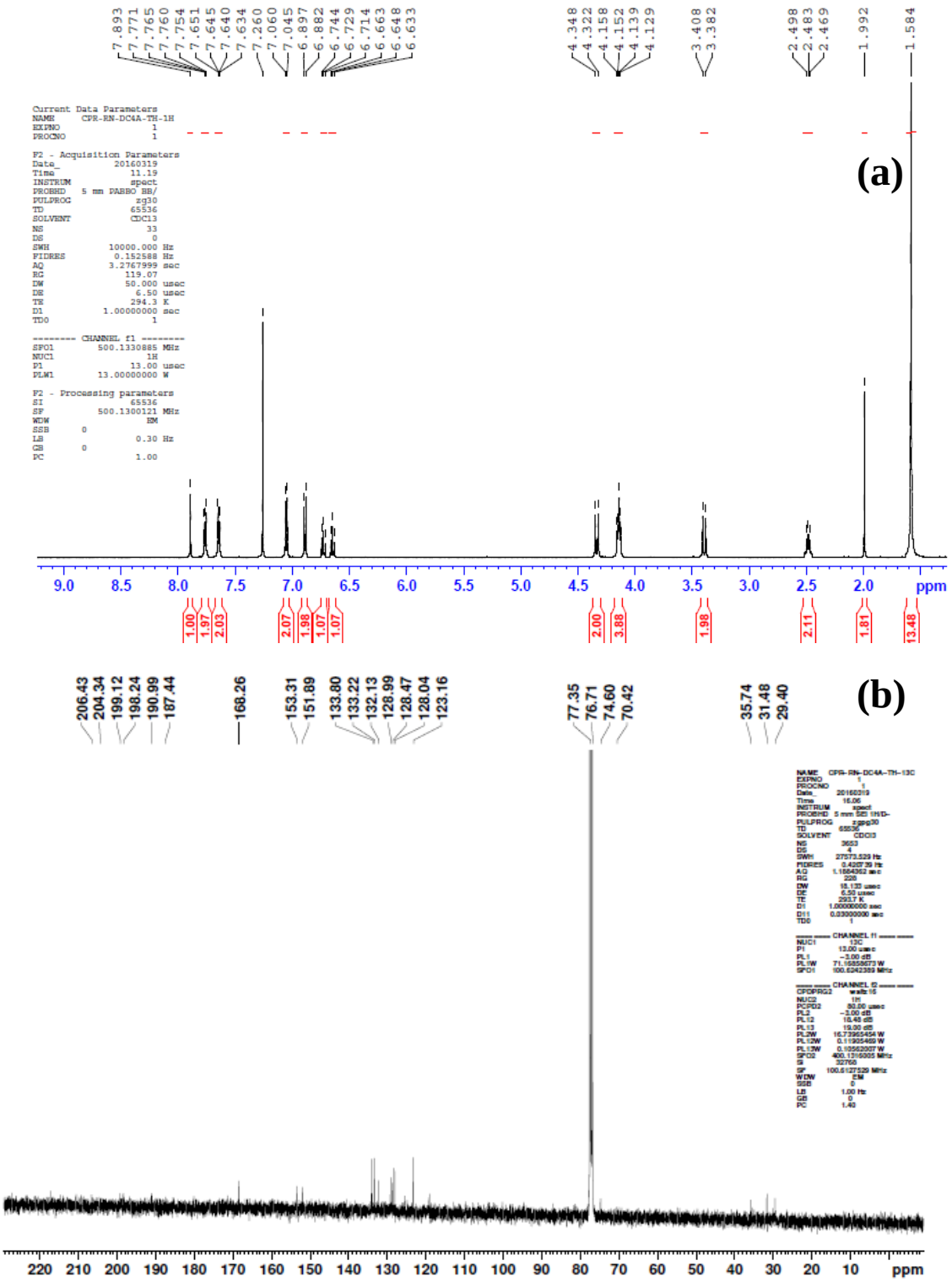

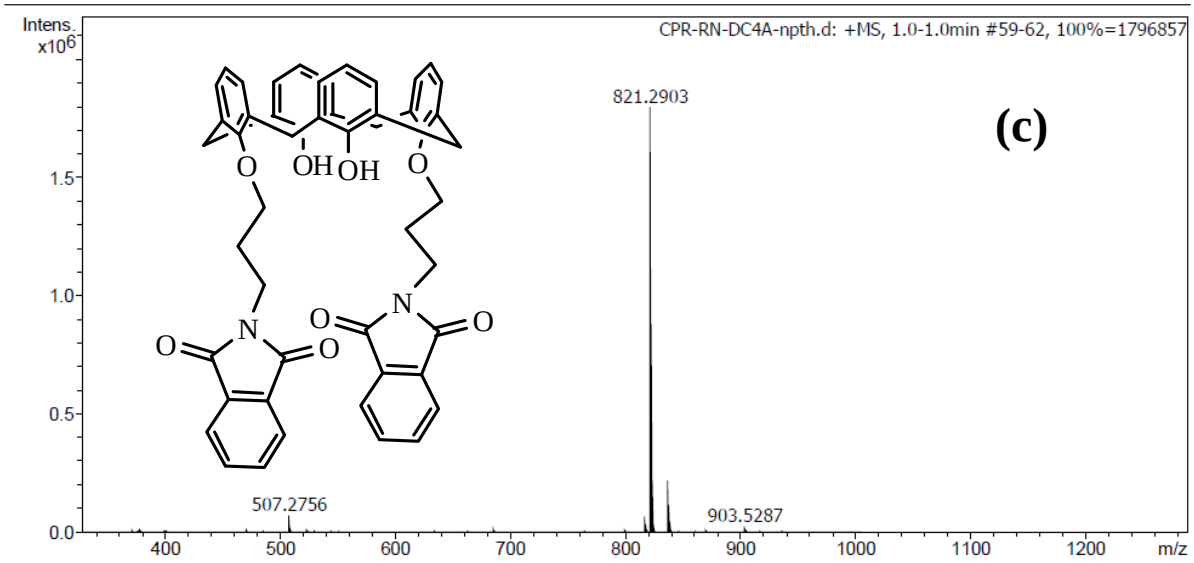

Figure S1. (a) ^{1}H, (b) ^{13}C NMR spectra of $\mathbf{P_3}$ in $CDCl_3$ and (c) ESI-MS spectrum of $\mathbf{P_3}$.

S2. Spectra for **P_4**.

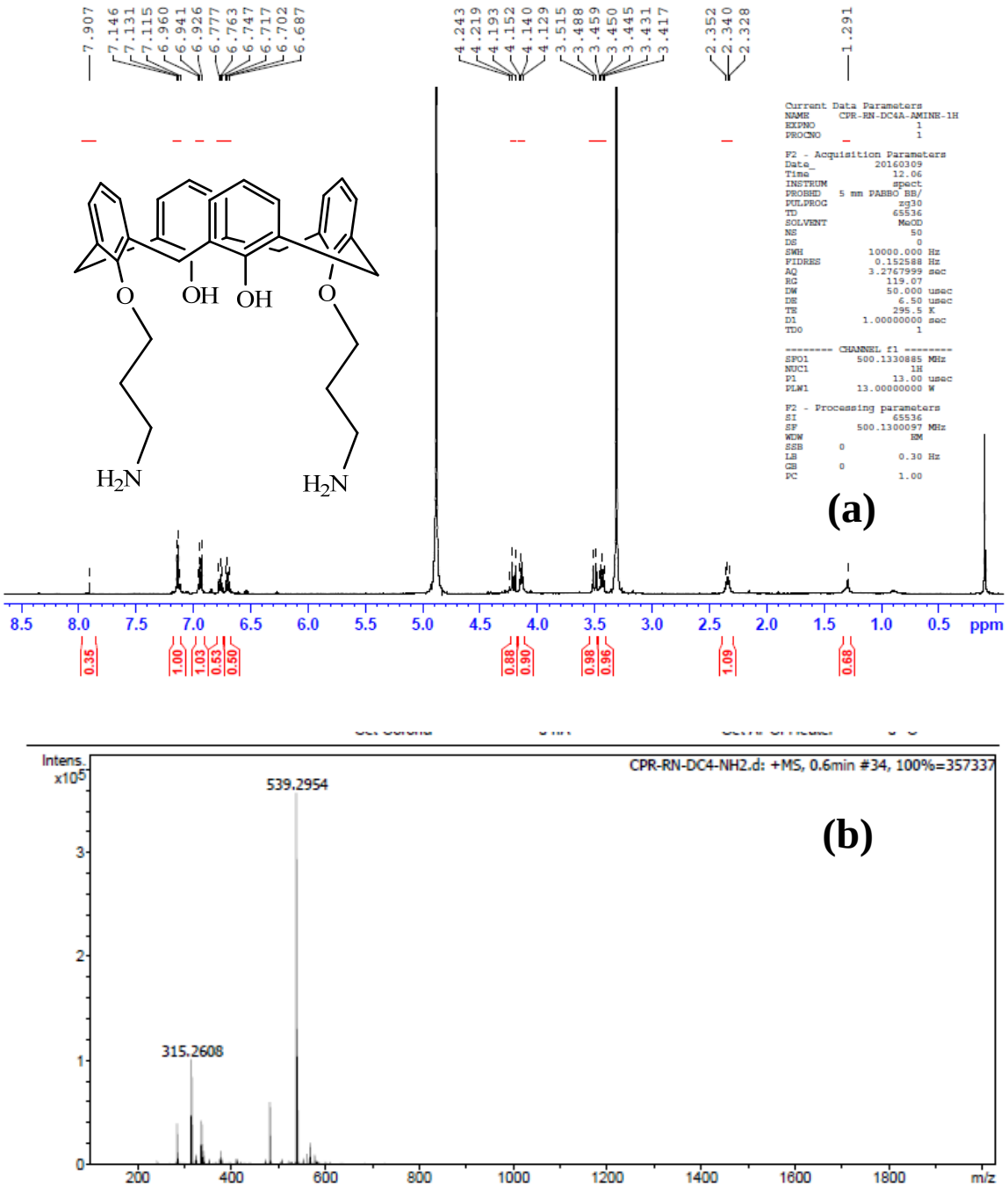

Figure S2. (a) ^{1}H NMR and (b) ESI-MS spectra for **P_4**.

S3. Spectra for $\mathbf{P_5}$.

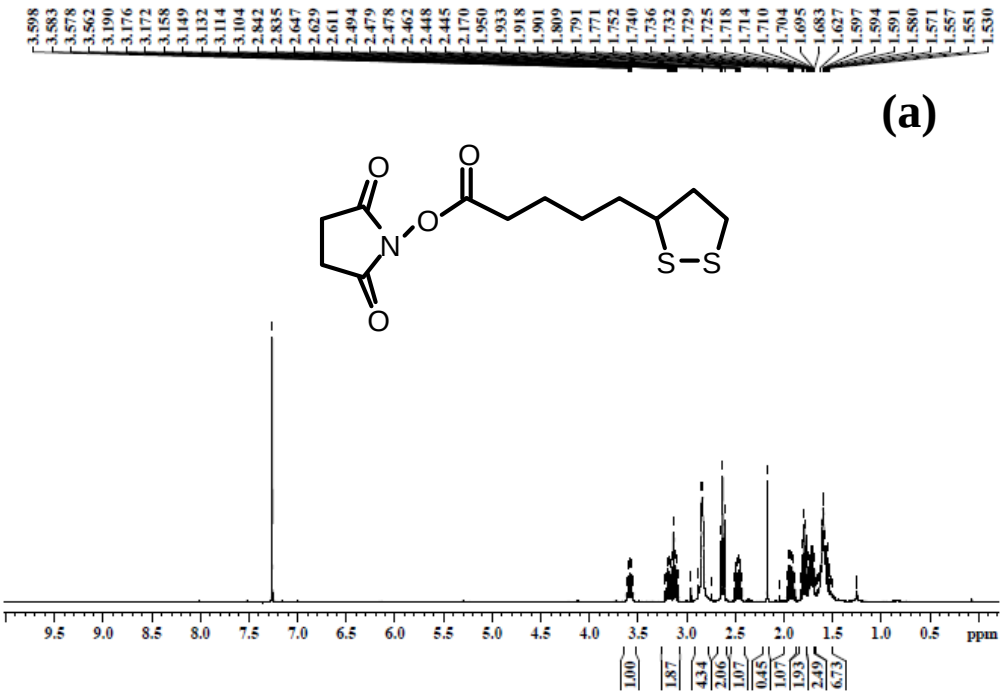

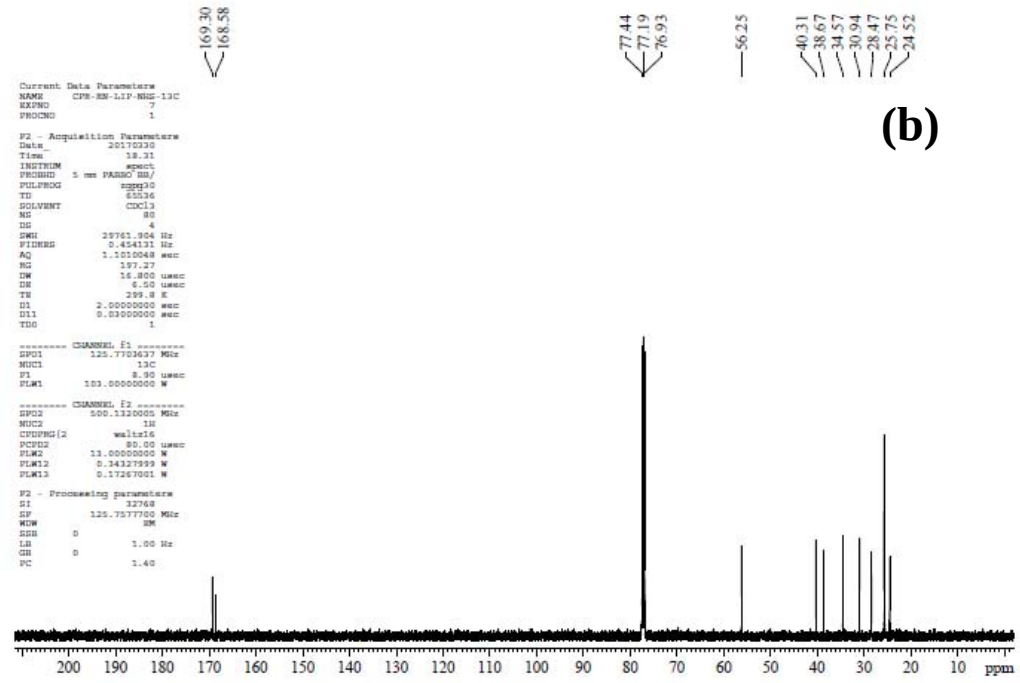

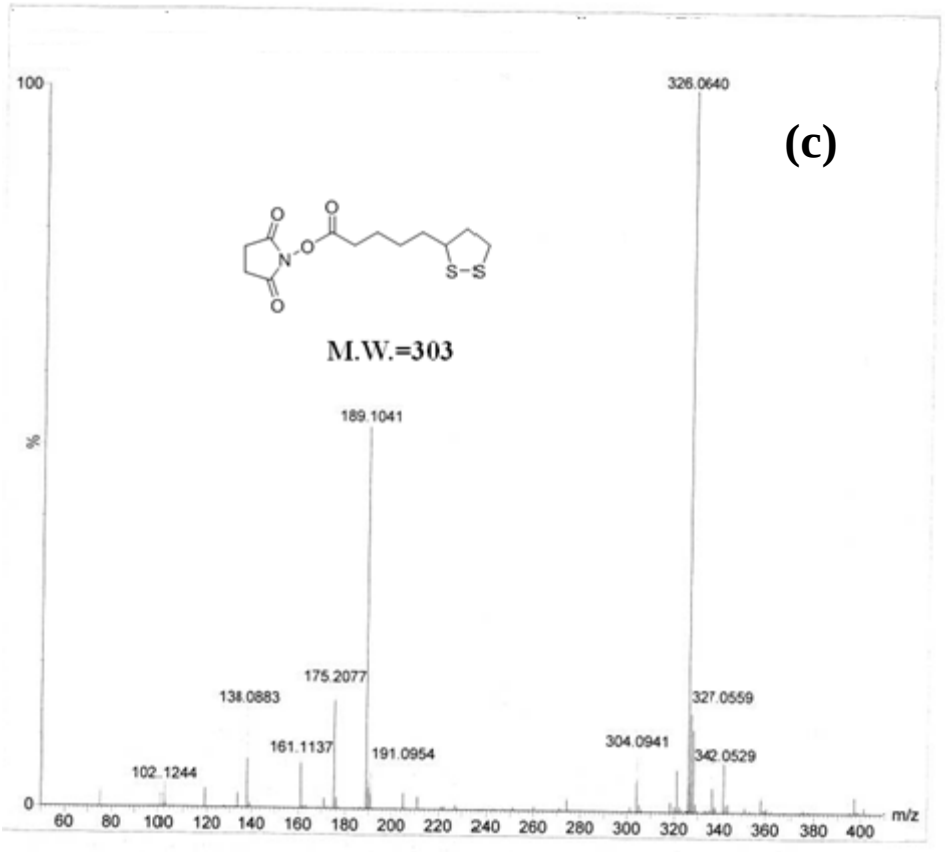

Figure S3. (a) ^{1}H & (b) ^{13}C NMR and (c) ESI-MS spectra for **P_5**.

S4. Spectra for **L**.

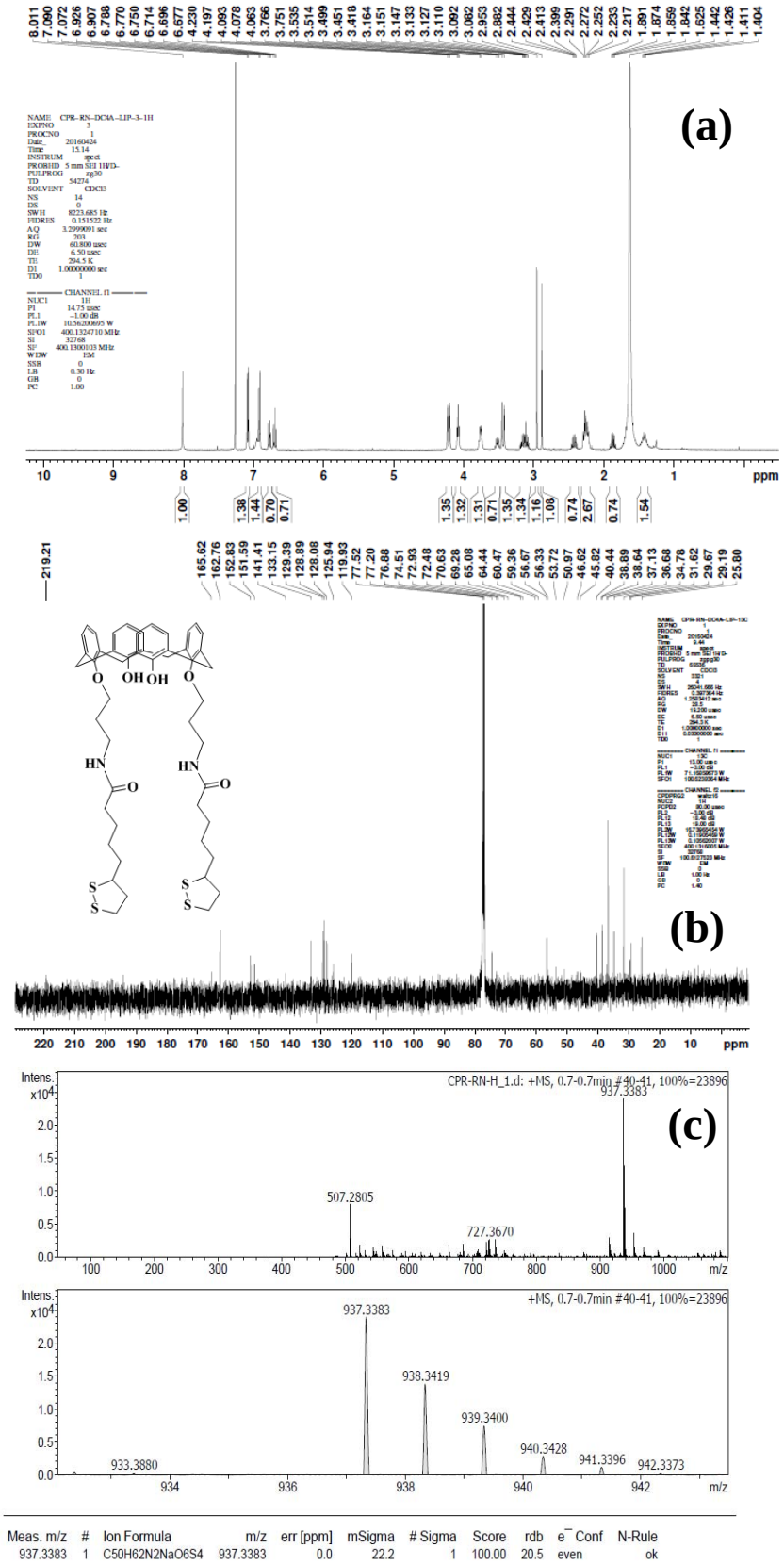

Meas. m/z	#	Ion Formula	m/z	err [ppm]	mSigma	# Sigma	Score	rdb	e⁻ Conf	N-Rule
937.3383	1	C50H62N2NaO6S4	937.3383	0.0	22.2	1	100.00	20.5	even	ok

Figure S4. (a) ^{1}H & (b) ^{13}C NMR and (c) ESI-MS spectra for **L**.

S5. Spectra for $\mathbf{R_2}$.

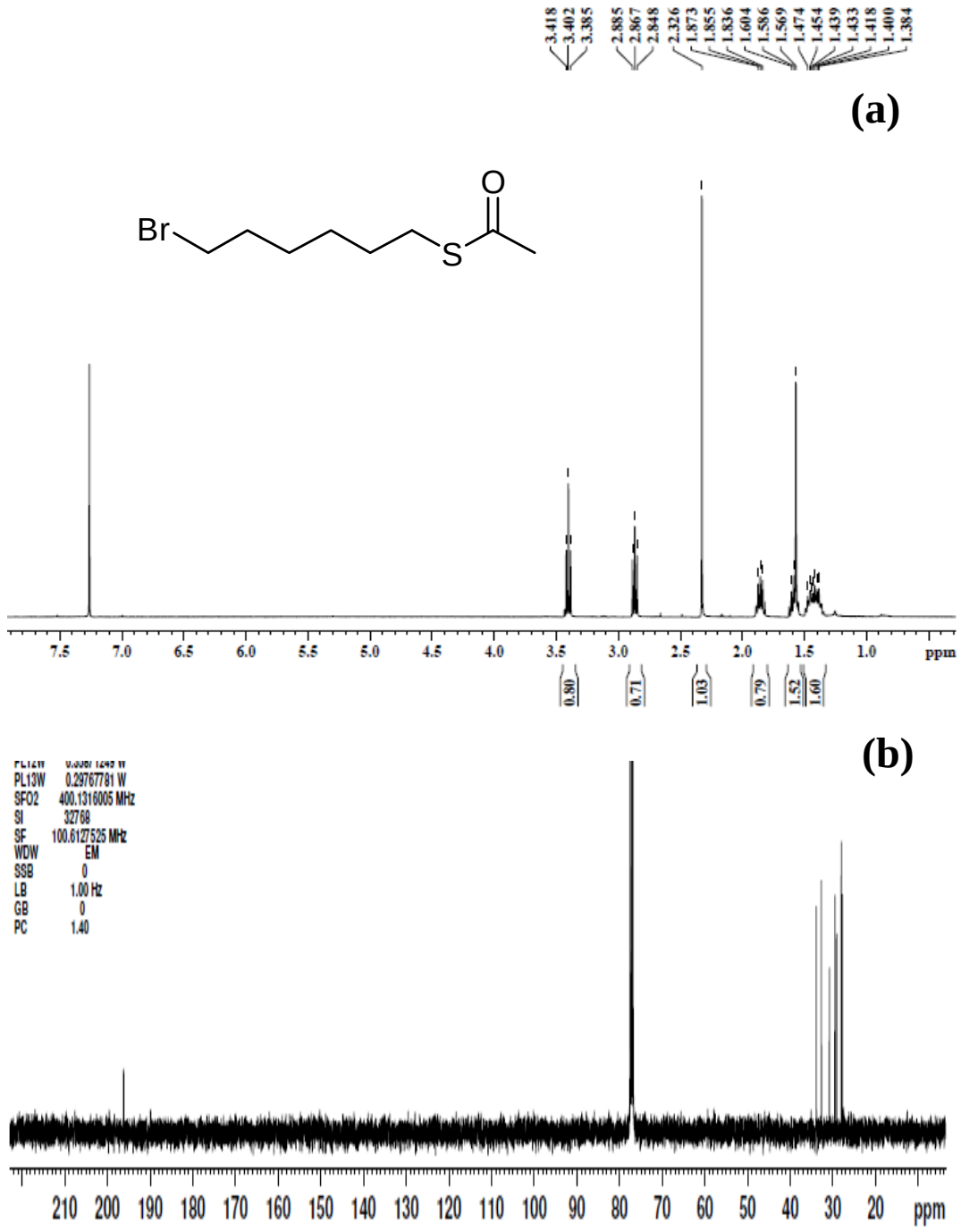

Figure S5. (a) ^{1}H & (b) ^{13}C NMR spectra for $\mathbf{R_2}$.

S6. Spectra for **Py-SAc**.

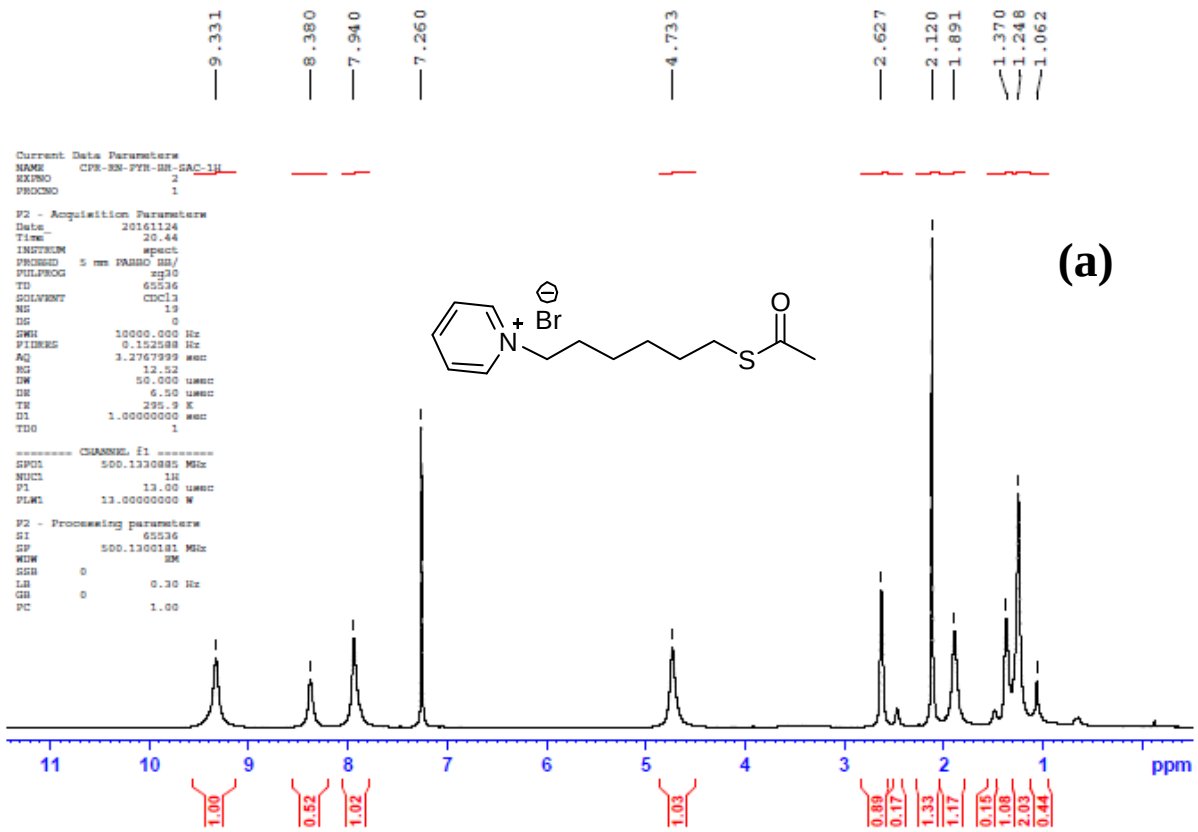

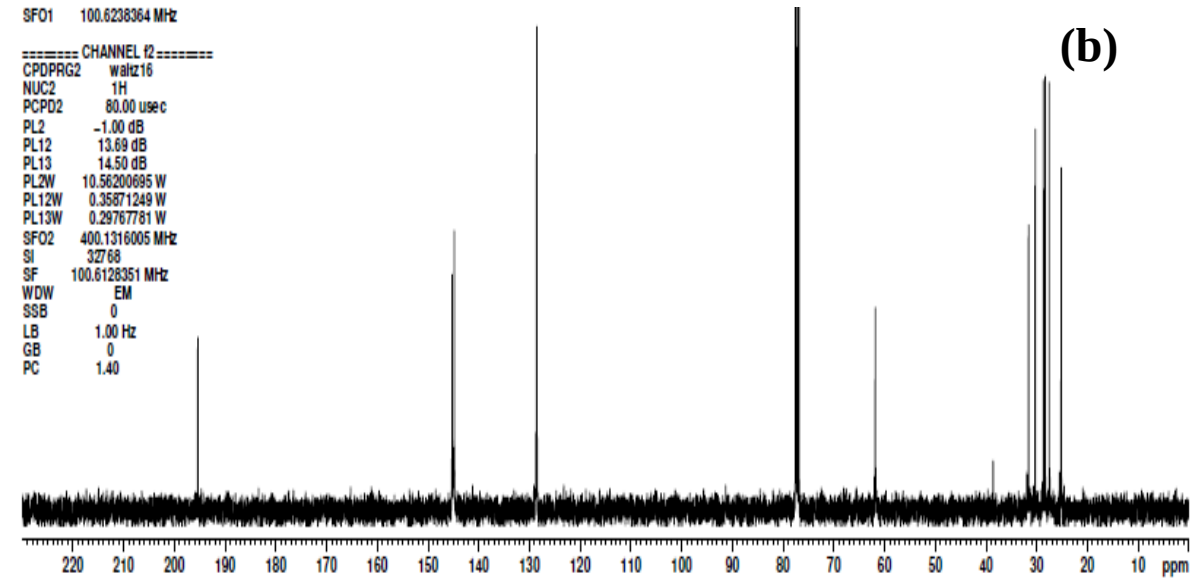

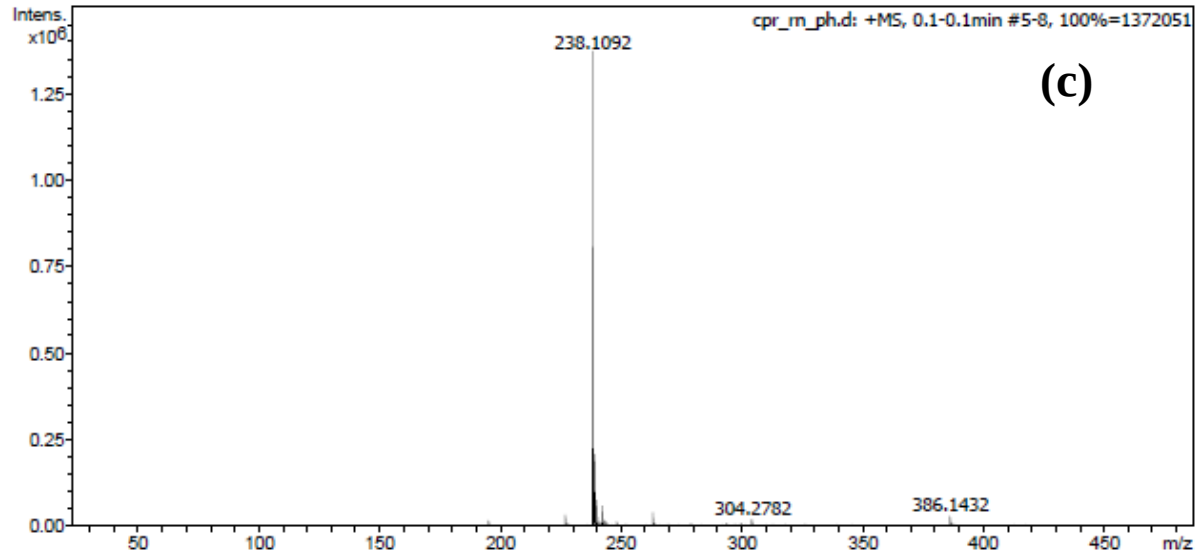

Figure S6. (a) ^{1}H & (b) ^{13}C NMR and (c) ESI-MS spectra for **Py-SAc**.

S7. **L** and **CPC** functionalization onto **GNR**.

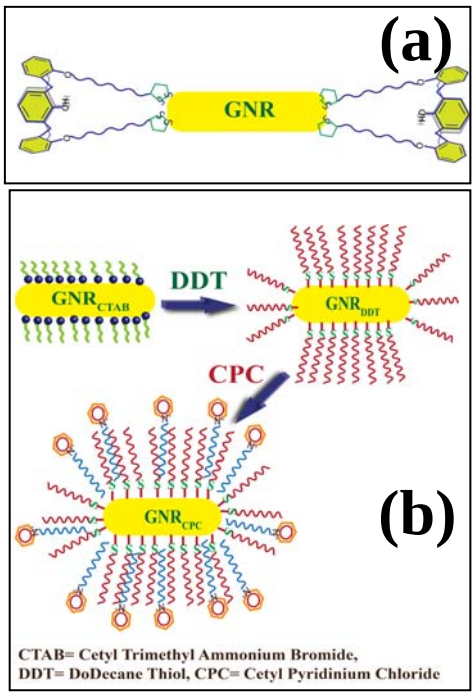

Figure S7. Schematic representation of **L** and **CPC** functionalization of **GNR**.

S8. XPS spectra of **Py-SAc** and **$GNR_{Py\text{-}SAc}$**.

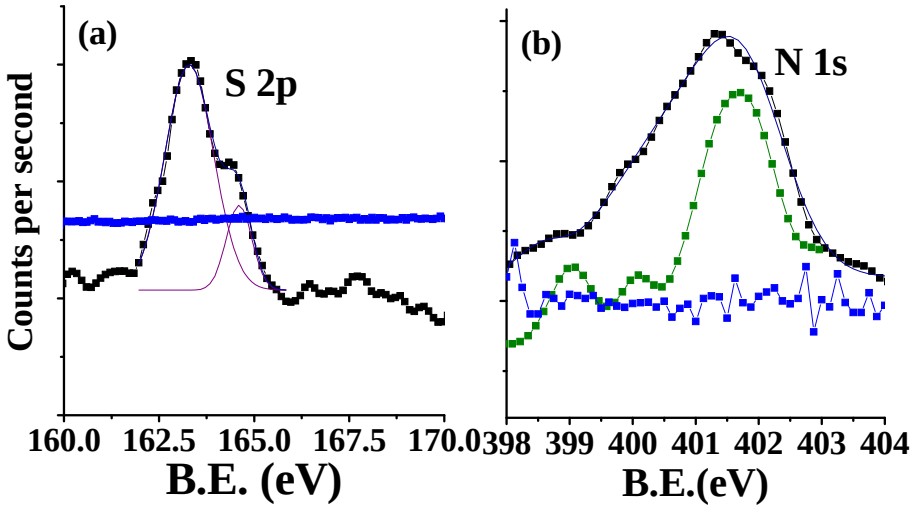

Figure S8. XPS spectra of **GNR**, **Py-SAc** and **$GNR_{Py\text{-}SAc}$** : (a) S 2p and (b) N 1s. The color code: **GNR** (**blue**), **Py-SAc** (**green**) & **$GNR_{Py\text{-}SAc}$** (**black**).

S9. TEM micrograph of **GNR_{CPC}**.

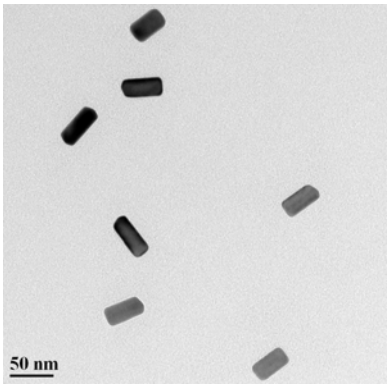

Figure S9. TEM micrograph of **GNR_{CPC}**.

S10. Schematic showing possible mode of interaction between **GNR_L** and **$GNR_{Py\text{-}SAc}$**.

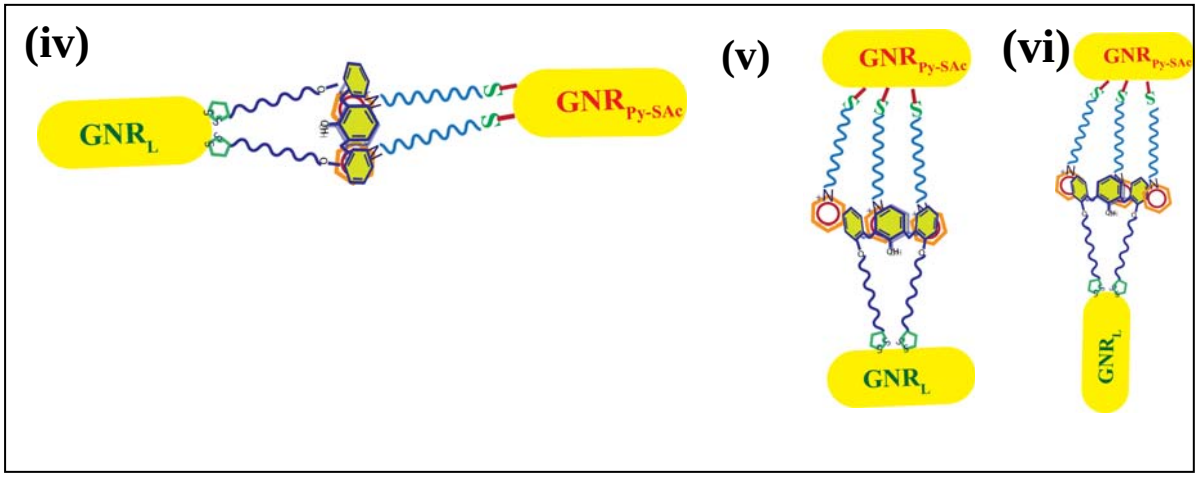

Figure S10. Representation of different modes of interaction between **GNR_L** and **$GNR_{Py\text{-}SAc}$**.

S11. MTT assay data.

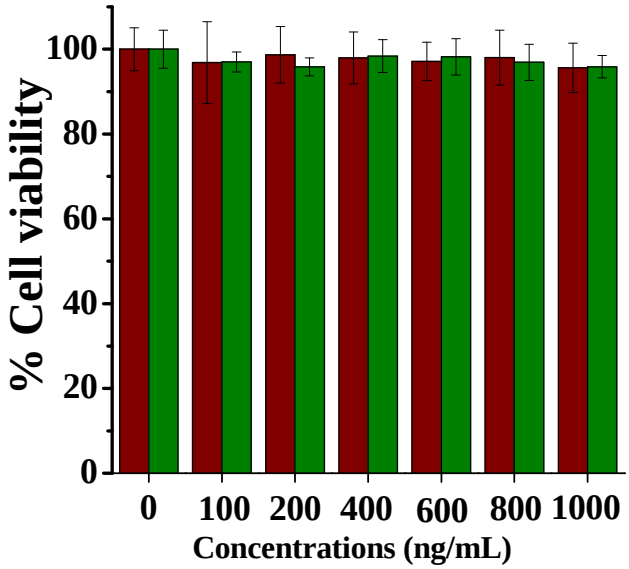

Figure S11. MTT assay of HeLa cells treated with different concentrations of **L** (**brown**), and **Py-SAc** (**green**) (0 to 1000 ng/mL) for 24 h incubation.

S12. IC_{50} value from MTT assay data.

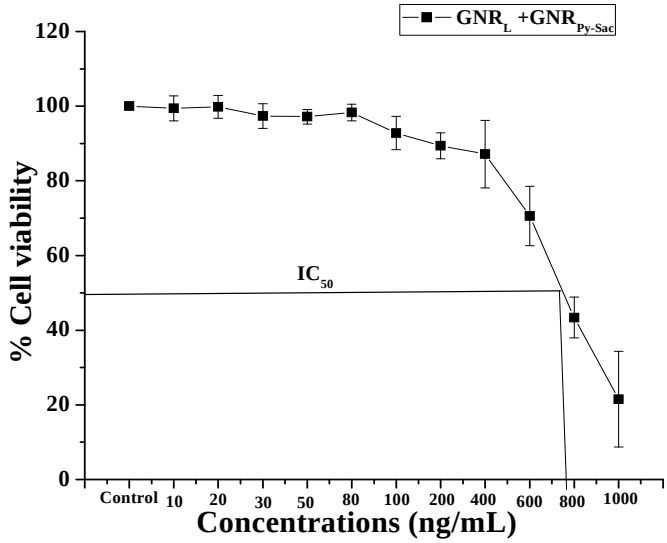

Figure S12. IC_{50} value calculated from MTT assay of HeLa cells treated with different concentrations of {$\mathbf{GNR_L}$+$\mathbf{GNR_{Py\text{-}SAc}}$} (0 to 1000 ng/mL) for 24 h incubation.

S13.Cell imaging data from fluorescence microscopy.

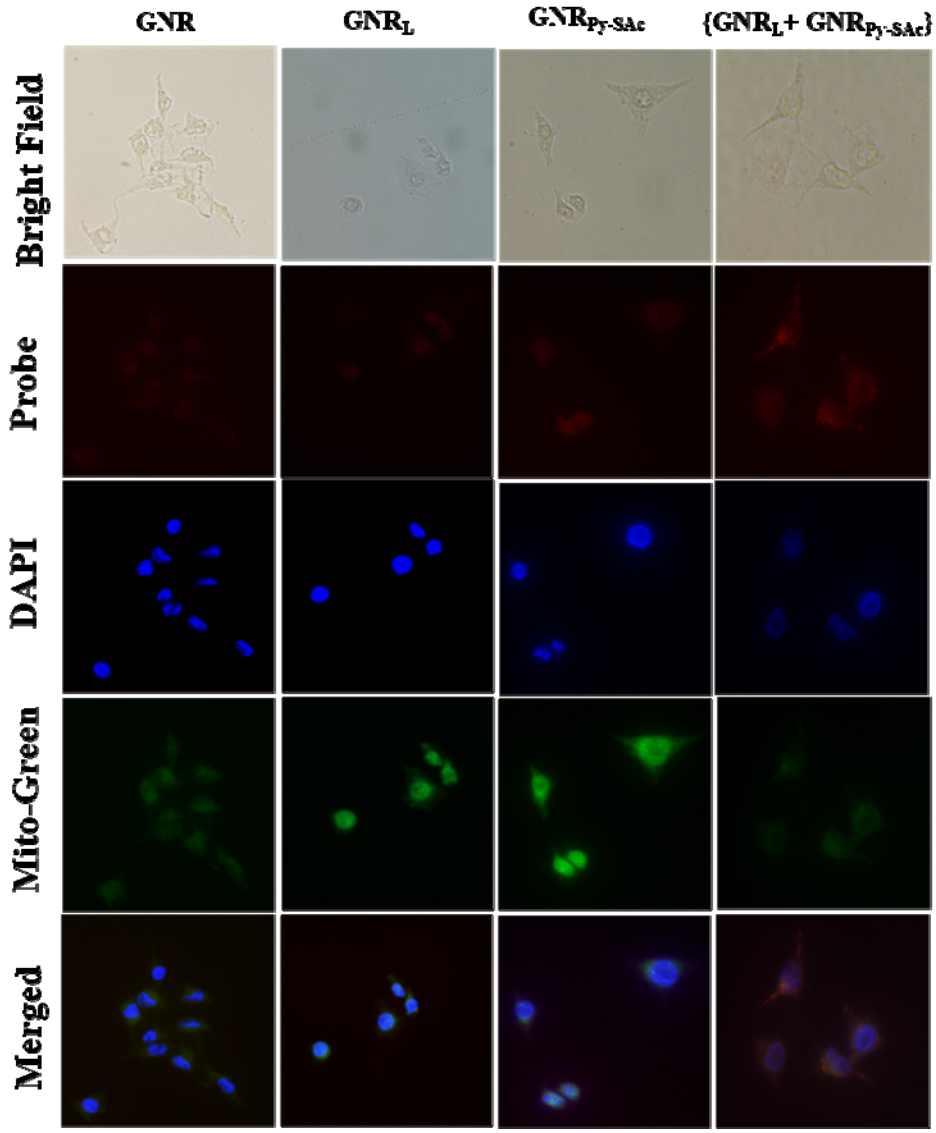

Figure S13. Fluorescence microscopy images of HeLa cell treated with 800ng/mL of **GNR, GNR$_L$, GNR$_{Py-SAc}$** and **{GNR$_L$+GNR$_{Py-SAc}$}**. The emission of the red fluorescence is from the probe, **{GNR$_L$+GNR$_{Py-SAc}$}**; the blue fluorescence from DAPI and the green fluorescence from mito-tracker green.

S14. Table S1. Co-localization parameters of {**GNR_L+GNR_{Py-SAc}**} of mito-tracker green and **GNR**.

Co-localization Parameter	Range	Value	% Co-localization
Pearson's coefficient	**-1:+1**	**0.603**	**60.3**
Overlap co-efficient	**-1:1**	**0.953**	**95.3**
Li's ICQ	**-0.5:0.5**	**0.348**	**69.6**
Manders M1/M2	**0:1**	**0.447** **0.294**	**44.7** **29.4**
Correlation coefficient	**-1:1**	**0.603**	**60.3**
Van Steensel's Cross-correlation Coefficient	**0:1**	**0.458 (obtained for dx=-20) CCF max.: 0.603**	**60.3**

S15. Stability study of **GNR**-nano-composites.

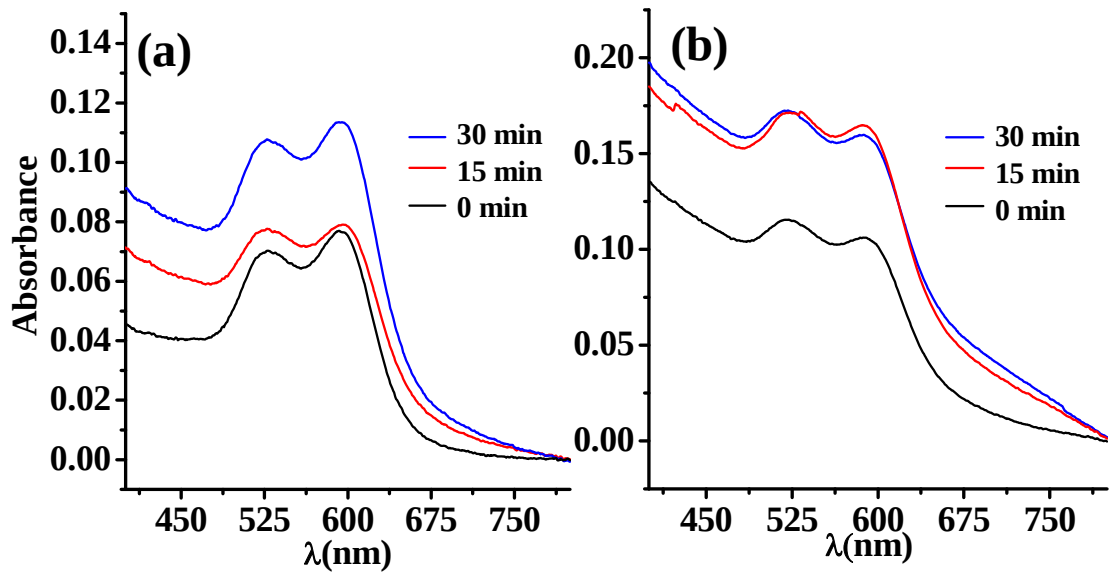

Figure S14. Stability analysis of (a) $\mathbf{GNR_{Py\text{-}SAc}}$ and (b) {$\mathbf{GNR_{L}}$+$\mathbf{GNR_{Py\text{-}SAc}}$} upon laser irradiation for 0, 15 and 30 minutes.

S16. Laser induced cancer cell cytotoxicity of HeLa cells by PI staining using Fluorescence microscopy analysis.

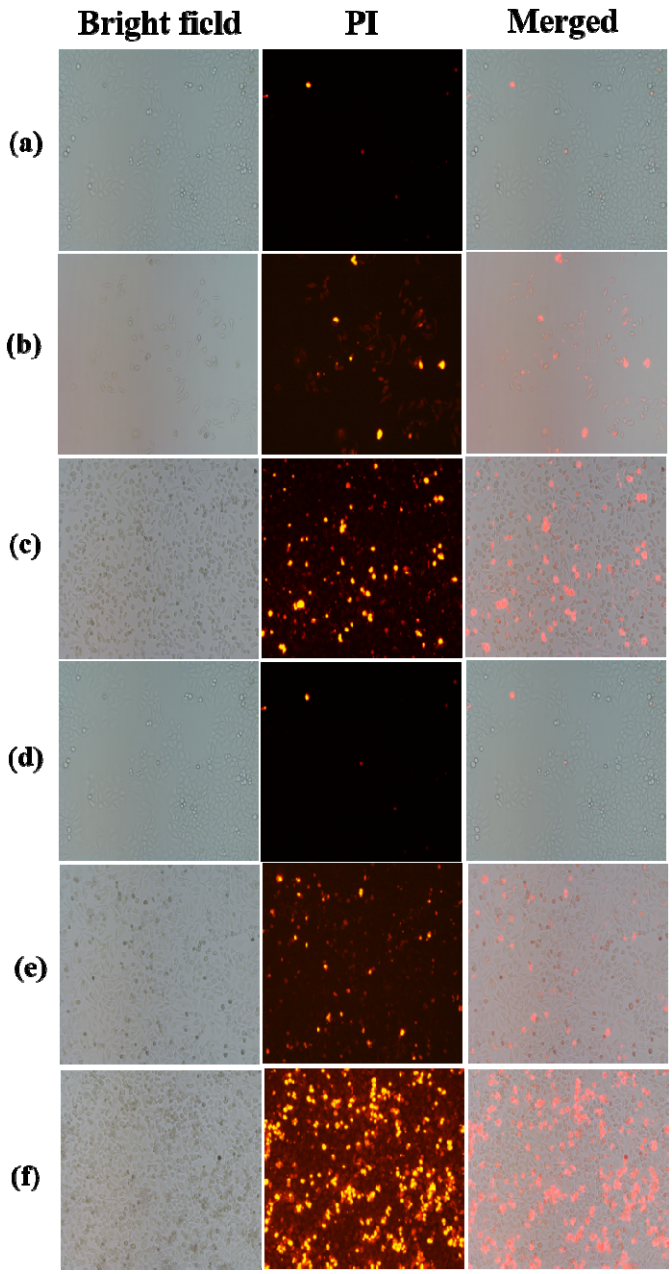

Figure S15. Fluorescence microscopy images of propidium iodide stained HeLa cells after laser treatment with 500ng/mL of $\mathbf{GNR_{Py\text{-}SAc}}$ and {$\mathbf{GNR_L}$+$\mathbf{GNR_{Py\text{-}SAc}}$}. (a) and (d) untreated HeLa cells. The cells incubated with (b) $\mathbf{GNR_{Py\text{-}SAc}}$ and (c) {$\mathbf{GNR_L}$+$\mathbf{GNR_{Py\text{-}SAc}}$} respectively and irradiated for 1 min; (e) $\mathbf{GNR_{Py\text{-}SAc}}$ and (f) {$\mathbf{GNR_L}$+$\mathbf{GNR_{Py\text{-}SAc}}$} respectively and irradiated for 3 min.

S17. Laser induced cell death in HeLa cells using FACS analysis.

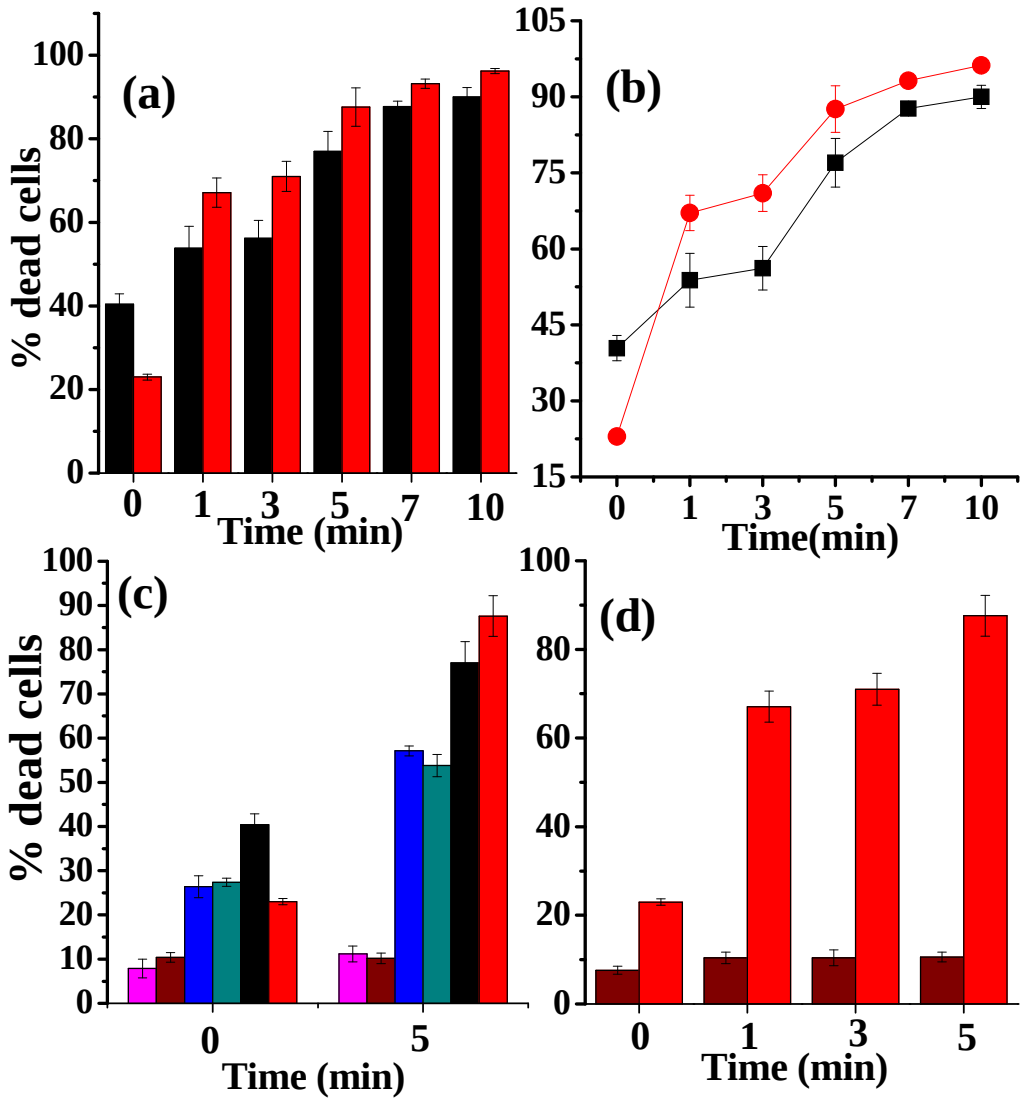

Figure S16. The percentage of dead cells obtained by FACS analysis in the HeLa cells treated with (a) and (b) **$GNR_{Py\text{-}SAc}$** (**black**) and {**GNR_L**+**$GNR_{Py\text{-}SAc}$**} (**red**) for different time of laser irradiation. (c) control (**pink**), **L** (**brown**), **GNR** (**blue**), **GNR_L** (**green**), **$GNR_{Py\text{-}SAc}$** (**black**) and {**GNR_L**+**$GNR_{Py\text{-}SAc}$**} (**red**) for 0 and 5 min of laser irradiation; and (d) **L** (**brown**) and {**GNR_L**+**$GNR_{Py\text{-}SAc}$**} (**red**) for 0, 1, 3 and 5 min with 633 nm laser.